NASA/TM-2002-211645
ARL-TR-2711

Failure Analysis of a Helicopter External Fuel-Tank Pylon

John A. Newman
U.S. Army Research Laboratory
Vehicle Technology Directorate
Langley Research Center, Hampton, Virginia

Robert S. Piascik
Langley Research Center, Hampton, Virginia

Richard A. Lindenberg
U.S. Coast Guard Aircraft Repair and Supply Center
Elizabeth City, North Carolina

April 2002

The NASA STI Program Office ... in Profile

Since its founding, NASA has been dedicated to the advancement of aeronautics and space science. The NASA Scientific and Technical Information (STI) Program Office plays a key part in helping NASA maintain this important role.

The NASA STI Program Office is operated by Langley Research Center, the lead center for NASA's scientific and technical information. The NASA STI Program Office provides access to the NASA STI Database, the largest collection of aeronautical and space science STI in the world. The Program Office is also NASA's institutional mechanism for disseminating the results of its research and development activities. These results are published by NASA in the NASA STI Report Series, which includes the following report types:

- TECHNICAL PUBLICATION. Reports of completed research or a major significant phase of research that present the results of NASA programs and include extensive data or theoretical analysis. Includes compilations of significant scientific and technical data and information deemed to be of continuing reference value. NASA counterpart of peer-reviewed formal professional papers, but having less stringent limitations on manuscript length and extent of graphic presentations.

- TECHNICAL MEMORANDUM. Scientific and technical findings that are preliminary or of specialized interest, e.g., quick release reports, working papers, and bibliographies that contain minimal annotation. Does not contain extensive analysis.

- CONTRACTOR REPORT. Scientific and technical findings by NASA-sponsored contractors and grantees.

- CONFERENCE PUBLICATION. Collected papers from scientific and technical conferences, symposia, seminars, or other meetings sponsored or co-sponsored by NASA.

- SPECIAL PUBLICATION. Scientific, technical, or historical information from NASA programs, projects, and missions, often concerned with subjects having substantial public interest.

- TECHNICAL TRANSLATION. English-language translations of foreign scientific and technical material pertinent to NASA's mission.

Specialized services that complement the STI Program Office's diverse offerings include creating custom thesauri, building customized databases, organizing and publishing research results ... even providing videos.

For more information about the NASA STI Program Office, see the following:

- Access the NASA STI Program Home Page at ***http://www.sti.nasa.gov***

- E-mail your question via the Internet to help@sti.nasa.gov

- Fax your question to the NASA STI Help Desk at (301) 621-0134

- Phone the NASA STI Help Desk at (301) 621-0390

- Write to:
  NASA STI Help Desk
  NASA Center for AeroSpace Information
  7121 Standard Drive
  Hanover, MD 21076-1320

NASA/TM-2002-211645
ARL-TR-2711

Failure Analysis of a Helicopter External Fuel-Tank Pylon

John A. Newman
U.S. Army Research Laboratory
Vehicle Technology Directorate
Langley Research Center, Hampton, Virginia

Robert S. Piascik
Langley Research Center, Hampton, Virginia

Richard A. Lindenberg
U.S. Coast Guard Aircraft Repair and Supply Center
Elizabeth City, North Carolina

National Aeronautics and
Space Administration

Langley Research Center
Hampton, Virginia 23681-2199

April 2002

Available from:

NASA Center for AeroSpace Information (CASI)
7121 Standard Drive
Hanover, MD 21076-1320
(301) 621-0390

National Technical Information Service (NTIS)
5285 Port Royal Road
Springfield, VA 22161-2171
(703) 605-6000

Abstract

An eight-inch-long (0.2 m) crack was found in an external helicopter fuel-tank pylon. The damaged pylon was removed from service and analyzed at NASA Langley Research Center to determine the cause of the crack. Results of the analysis revealed that crack initiation occurred at corrosion pits in a fastener hole and crack propagation was a result of fatigue loading.

Introduction

At the U.S. Coast Guard air station in Elizabeth City, North Carolina, an eight-inch-long (0.2 m) crack was found in an external fuel-tank pylon of a HH-60 "Jayhawk" helicopter. External fuel tanks are used to extend the range and operation times of U.S. Coast Guard (USCG) helicopters and are fastened to pylons attached to the helicopter fuselage. Fuel-tank pylons are fabricated from 7075 aluminum alloy forgings that are machined into the final configuration. The HH-60 is capable of carrying three external pylon-drop fuel tanks: one 80-gallon (300 L) tank and two 120-gallon (450 L) tanks. The crack was found in a 120-gallon tank pylon. Photographs of a Coast Guard HH-60 helicopter are shown in Figure 1. The photograph of the entire helicopter fuselage in part (a) shows the location of a 120-gallon fuel tank. As seen in part (b), the pylon that connects the fuel-tank assembly to the fuselage is normally covered and hidden from view. A photograph of a fuel-tank pylon is shown mounted to the fuselage in part (c); the pylon is visible because the covering has been removed for inspection.

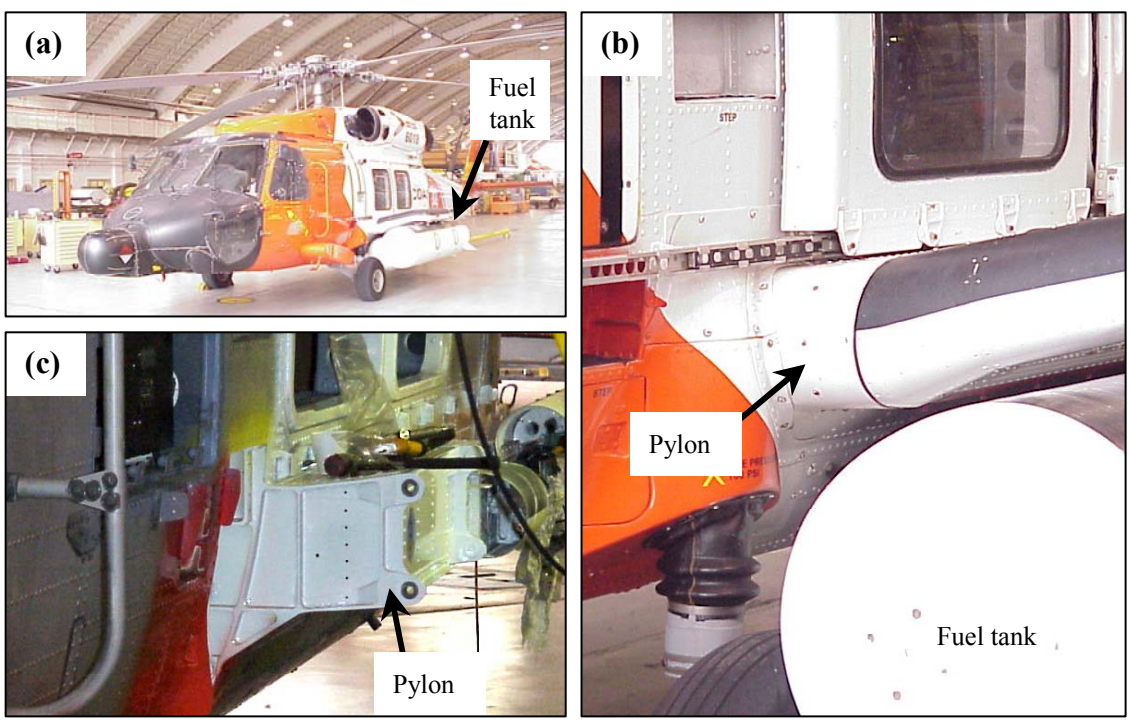

Figure 1. Photographs are shown of the external pylon-mounted fuel-tank assembly on the HH-60 helicopter. (a) A 120-gallon fuel tank is shown on the fuselage. (b) A more detailed photograph of the fuel-tank pylon attachment is shown. (c) A pylon is seen after the fuel-tank assembly was removed for inspection.

The failure analysis reported herein concentrated on finding evidence of fatigue loading and/or corrosion that could lead to cracking of the fuel-tank pylon. Helicopter components are known to experience fatigue (cyclic) loading resulting in possible fatigue cracking (refs. 1, 2). Additionally, USCG helicopters are routinely exposed to corrosive marine environment and cracking may be exacerbated by environmental-load interactions that produce brittle crack growth resulting from stress corrosion cracking and/or corrosion fatigue (ref. 3). After the crack was detected, the damaged pylon was removed from service and shipped to NASA Langley Research Center in Hampton, Virginia for detailed destructive examinations to determine the cause of cracking.

Initial Visual Inspection

A photograph of the cracked pylon is shown as Figure 2a. The left curved-side of the pylon was mounted vertically to the helicopter fuselage; the arrow in the upper-right corner of Figure 2a indicates the vertical-up direction. The fuel-tank assembly was attached to the pylon through the two holes on the far right side of Figure 2a. Loads applied to the pylon are nominally expected in the vertically downward direction, applied at the end of the horizontal (cantilever) portion of the pylon, creating high bending stresses in the corner region of the pylon as indicated in Figure 2a. The crack appears to have initiated at fastener holes in this high stress region and propagated in a vertically downward direction. Eventually the crack propagated into a vertical stiffener and appeared to have arrested. Figure 2b is a more detailed view of the crack region outlined in Figure 2a. The dashed line in Figure 2b parallels the crack from the apparent region of crack initiation (fastener holes in the upper flange) to crack arrest at a vertical stiffener.

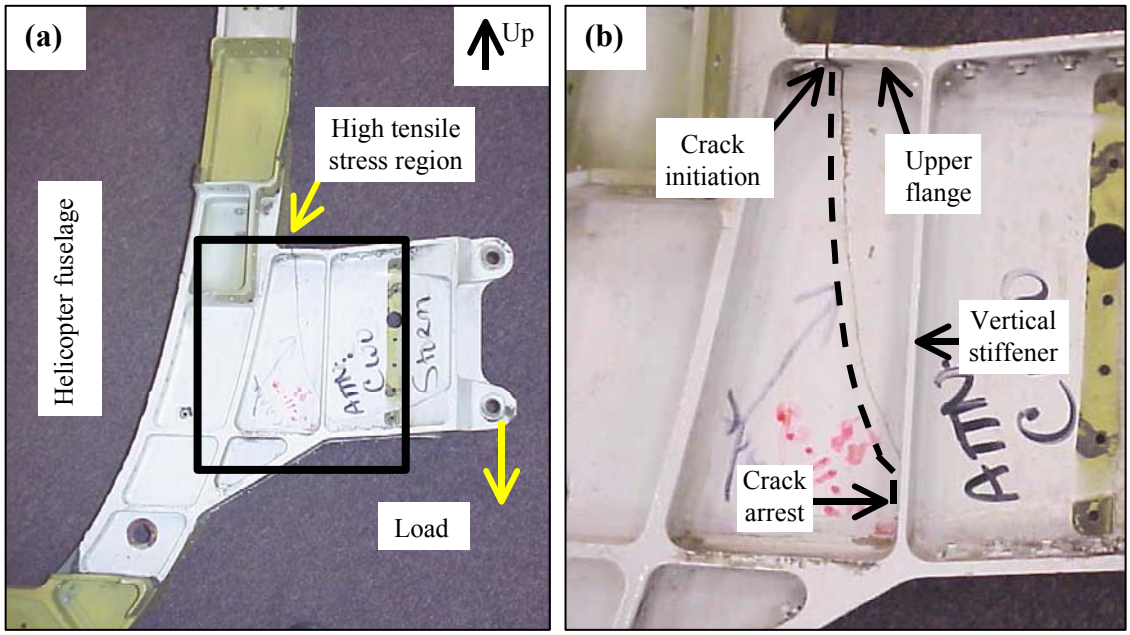

Figure 2. Photographs of the cracked pylon are shown. (a) A photograph of most of the pylon is shown. (b) A more detailed image is given of the cracked region.

The top of the pylon upper flange, in the crack initiation region, is shown in Figure 3a. Here, the crack is seen bisecting two fastener holes, each $^{3}/_{16}$-inch (4.8 mm) in diameter; presumably, the crack initiated at one of these holes. The bottom surfaces of the upper flange near these fastener holes are shown in Figures 3b and 3c. The two smaller holes adjacent to the large hole located on the left of Figure 3a were used to attach the bracket shown in Figure 3b. Results presented later in this paper indicate that crack initiation occurred at the fastener hole shown in Figure 3b.

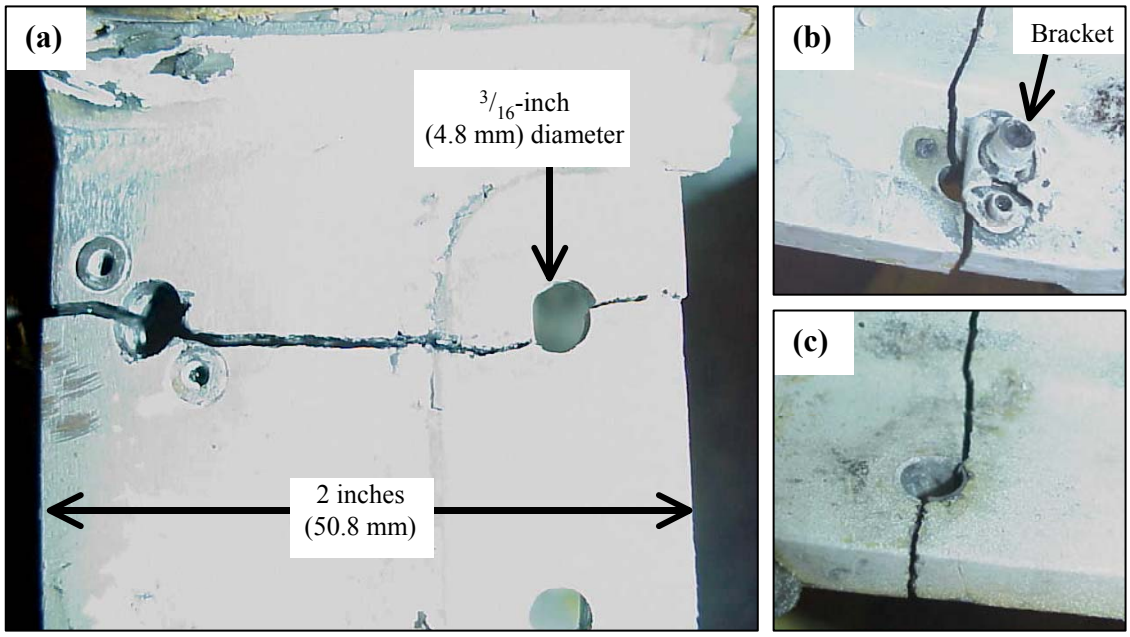

Figure 3. Photographs of the crack initiation region are shown. (a) A photograph of the crack intersecting two fastener holes on the top of the upper flange is shown. (b) The fastener hole on left of (a) is shown from the underside of the flange. (c) The fastener hole on right of (a) is shown from the underside of the flange.

Destructive Examination

To perform detailed examination of the crack surface, the pylon was broken by carefully applying a load at the end of the horizontal cantilever while the curved vertical portion was locked into position. This loading allowed the horizontal cantilevered portion of the pylon to rotate and fracture the remaining ligament without disturbing the crack surfaces. A photograph of the broken pylon is shown in Figure 4a. Only the crack surface associated with the smaller piece of the pylon was examined; the larger piece was preserved for future examination. A photograph of the crack surface in the upper flange (where crack

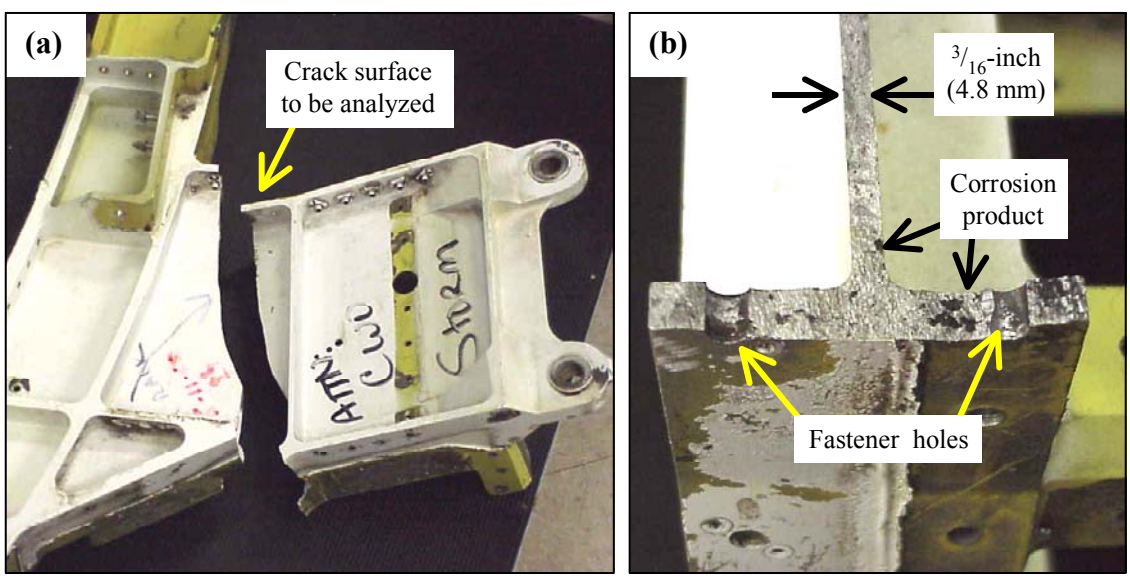

Figure 4. Photographs of the broken pylon are shown. (a) A photograph of the broken pylon is shown. (b) A detailed photograph is given of the crack surface in the crack initiation region.

initiation appeared to occur), and a portion of the web, is shown in Figure 4b. Visual inspection of the crack surfaces revealed dark-colored regions on the crack surfaces, primarily near the fastener holes where the crack appeared to initiate. These dark spots, indicated in Figure 4b, are corrosion products (likely oxide debris) that are typically produced during fatigue crack growth of aluminum alloys in an aggressive environment (refs. 4, 5). A photograph of the crack surface as it propagated from right to left into the vertical stiffener is shown in Figure 5. To the right of the curved final crack front, the fatigue crack surface is covered with a uniform dark colored corrosion product layer. To the left of the crack front, the fracture surface (produced as the cracked pylon was broken) is clean and free of corrosion products.

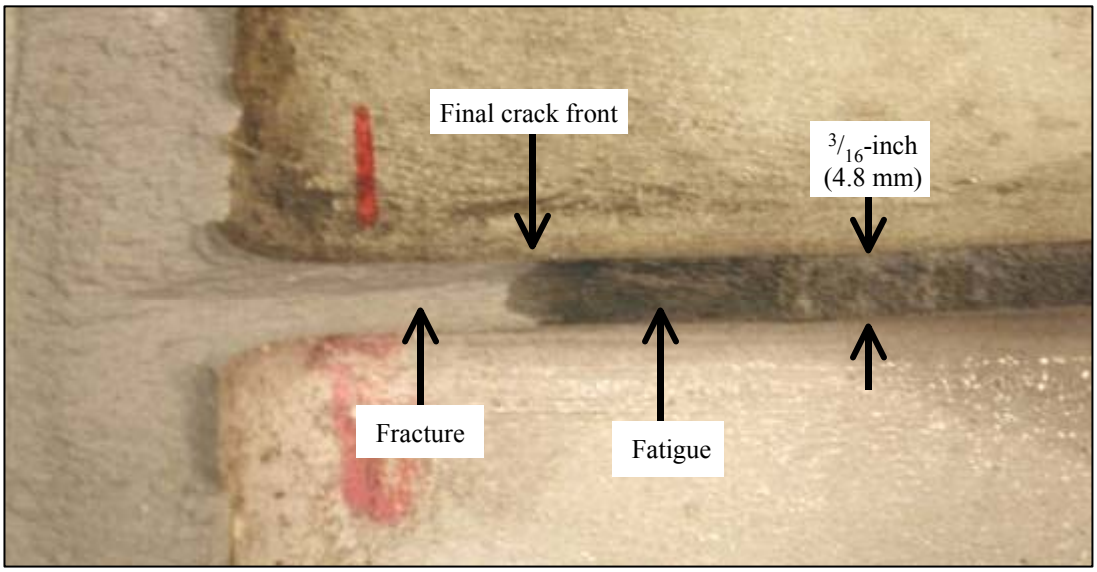

Figure 5. A photograph of the crack surface as the crack propagated into the vertical stiffener is shown.

Fractography

A more detailed examination of the crack surface was performed with a scanning electron microscope (SEM). The smaller piece of the broken pylon, shown in Figure 4a, was too large for SEM examination and was cut into smaller pieces. First, a single cut was made (indicated in Figure 6a by the dashed line) parallel to the crack so that the entire crack surface was contained in a strip of material approximately 12-inches (0.3 m) long. Five additional cuts were made normal to the crack surface (indicated in Figure 6b with dashed lines) dividing the crack surface into six pieces, each approximately 2-inches (50 mm) long. The six pieces of the crack surface were small enough to be accommodated in the SEM. Care was taken not to cut through regions containing important crack-surface features.

Crack-surface corrosion products made SEM analyses difficult. Therefore, the crack surface was ultrasonically cleaned in a 50% nitric acid (HNO_3) solution for 60-second intervals. After the crack surface was removed from the acid solution, it was thoroughly rinsed with water, and the cleaning procedure was repeated before the crack surface was thoroughly cleaned. (A third 60-second exposure was not needed.) This technique has been used at LaRC to remove oxides from crack surfaces without altering crack-surface features of interest.

Features and characteristics of the crack surface are used to provide information about the history and cause of the crack. The crack-surface features of primary interest to this study are markings that result from crack-tip deformation; herein, called deformation markings. Deformation markings are useful

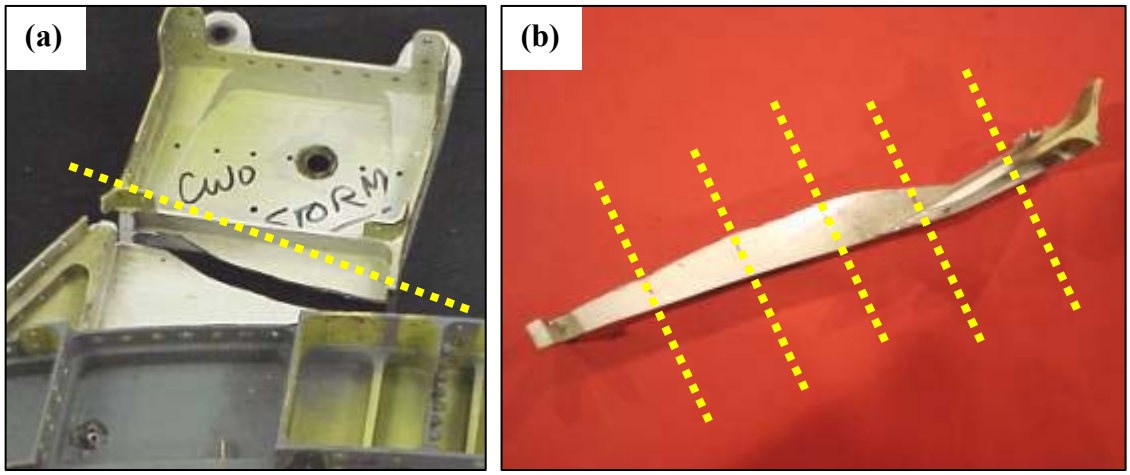

Figure 6. Two photographs are shown to illustrate how the broken pylon was cut for SEM analysis. (a) The first saw cut removed the crack surface from the pylon. (b) The crack surface was then cut into six smaller pieces.

because they indicate the location and shape of the crack front at an instant in time. Crack surfaces produced during constant-amplitude fatigue loading typically have periodic deformation markings that are nearly equally spaced (ref. 6). Where cracks are known to advance during each load cycle, the spacing between these markings (commonly called striations) is the increment of crack advance per load cycle, termed as the fatigue crack growth rate.* This is useful because the fatigue crack growth rate can be related to the crack-tip load parameter, ΔK. Most structures (including helicopter pylons) experience irregular variable-amplitude fatigue loading. Complex load interactions occur during variable-amplitude loading, possibly resulting in irregular fatigue crack growth rates or crack arrest (*i.e.*, cracks become non-propagating). In general, it is difficult to distinguish between striation markings (produced as a crack propagates) and crack arrest marks (produced as a crack arrests). Therefore, it is difficult to determine fatigue crack growth rates with deformation markings produced during variable-amplitude loading (ref. 9). Even in cases of complex variable-amplitude loading, a great deal of information about the crack history can be obtained from crack-surface markings. For example, both striations and crack arrest marks indicate the progression of the crack front, so no distinction between these markings is needed to determine the crack initiation site. During the early stages of crack growth, the crack propagates in radial directions from the crack initiation site producing curved crack-surface markings (concave toward the crack initiation site) that can be used to determine where crack initiation occurred.

SEM examination of the clean crack surface revealed crack-surface deformation markings, evidence that crack propagation was a result of fatigue loading. The majority of the crack surface did not exhibit deformation markings, but those that were found revealed that crack initiation occurred at corrosion pits in the fastener hole of Figure 3b. The photograph of the crack surface in Figure 7a shows the region of crack initiation; crack initiation occurred at the fastener hole in the upper right corner of the figure, highlighted with a box. The crack surface in Figure 7b is a higher-magnification image of the crack initiation region highlighted (box) in Figure 7a. A region of corrosion pitting is noted in Figure 7b along the inside edge of the fastener hole (right side of the photograph). The region of crack initiation noted in Figure 7b is shown at higher magnification in Figure 7c. Corrosion pits are seen as a rough-textured region on the right side of Figure 7c. Deformation markings on the crack surface are barely visible in Figure 7c. The curved dotted line in Figure 7c shows the curvature of the deformation marks (concave to

* For aluminum alloys, striated fatigue crack growth (one striation per load cycle) is known to occur for $\Delta K > 7$ MPa$\sqrt{m}$. Multiple load cycles may occur between crack-surface marks at lower ΔK (refs. 7, 8).

the right) indicating that crack initiation occurred at the corrosion pits seen on the right side of the figure. These marks are better seen at higher magnification in Figure 7d.

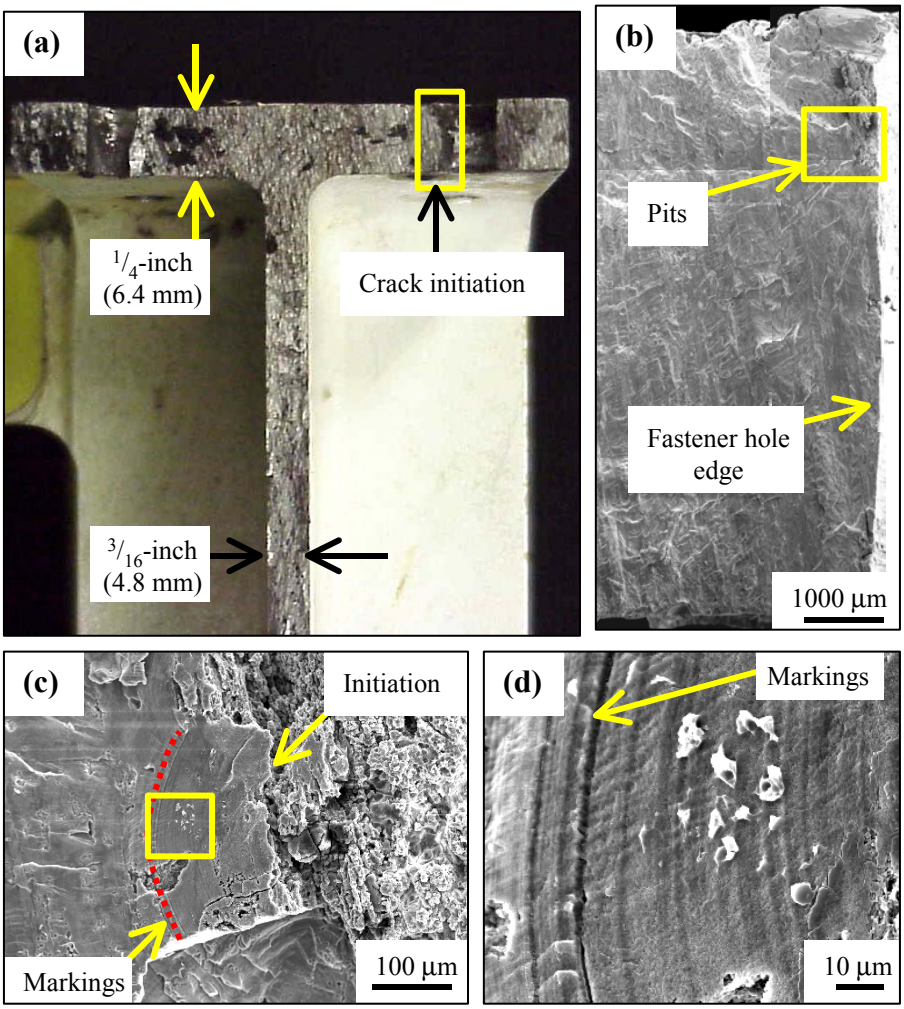

Figure 7. The crack initiation region is shown in a series of images, at increasing magnification. (a) Photograph of the crack surface in the pylon upper flange region is shown. Also shown are micrographs of (b) crack surface at edge of fastener hole surface, (c) crack initiation at corrosion pits, and (d) crack surface markings at high-magnification in crack initiation region.

SEM images of the crack initiation region of Figure 7 are shown at a different angle in Figure 8 to illustrate the complex nature of the crack surface and to highlight regions of pitting that did not result in crack initiation. Here, the crack surface was viewed at an angle 45° from the direction normal to the crack surface, and the specimen is rotated 90° (with respect to the orientation of Figure 7) so the fastener hole is oriented horizontally. In Figure 8a, the intersection of the crack surface with the edge of the fastener hole is indicated with a dashed horizontal line; the surface of the hole and the crack surface are below and above the dashed line, respectively. The upper and lower surfaces of the upper flange (shown in Figure 3) are the edges seen on the extreme right and left sides of Figure 8a, respectively. The boxes in Figure 8a identify two regions of corrosion pitting in the fastener hole: one where cracks did not initiate (left box) and one where cracks did initiate (right box). These regions are shown at higher magnification in Figures 8b and 8c, respectively.

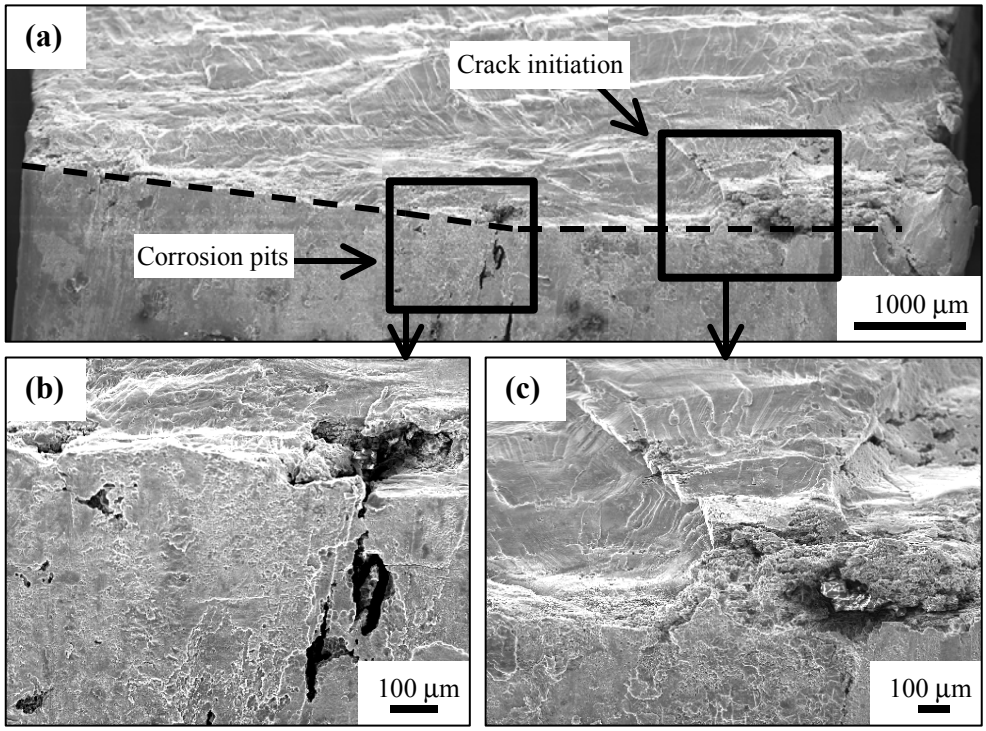

Figure 8. Micrographs of the crack initiation region, viewed at a 45° angle to the crack surface, are shown. (a) The crack surface at the edge of the fastener hole surface is shown. High-magnification micrographs are shown of corrosion pits (b) where cracks did not initiate and (c) where cracks initiation occurred.

Evidence of crack-surface deformation marks at three locations along the crack surface is shown in Figure 9. These three locations, identified in Figure 9a as b, c, and d, are shown at high-magnification in Figures 9b, 9c, and 9d, respectively. The markings observed in Figures 9b and 9c are not equally spaced, possibly suggesting that complex variable-amplitude loading occurred. The deformation markings shown in Figure 9d are equally spaced and exhibit the morphology typical of fatigue striations. The average spacing between deformation markings is determined by counting the number of marks intersecting lines along the crack growth direction (*i.e.* normal to the marks). In Figure 9b, 8 marks are counted along a line 100 μm long. For Figures 9c and 9d, 10 marks and 20 marks are counted along lines 15 μm and 30 μm long, respectively. If each deformation mark was produced by a single load cycle, the average fatigue crack growth rates corresponding to Figures 9b, 9c, and 9d would be 1.2 x 10^{-5} m/cycle, 1.5 x 10^{-6} m/cycle, and 1.5 x 10^{-6} m/cycle, respectively. The markings in Figures 9b and 9c are not regularly spaced and may not have been produced by single load cycles. Therefore, these markings do not permit a good estimation of fatigue crack growth rates. The crack-surface markings seen in Figure 9d are likely striations, each produced by a single load cycle. Therefore, the calculated fatigue crack growth rate of 1.5 x 10^{-6} m/cycle is likely a good estimate for the crack surface of Figure 9d. Based on laboratory 7075 aluminum data, the fatigue crack growth rate for Figure 9d corresponds to values of ΔK between 15 MPa√m and 20 MPa√m (refs. 10, 11).

Discussion

The results of detailed destructive examinations show that crack initiation occurred at corrosion pits that formed in a fastener hole. Corrosion problems are greater for USCG helicopters because they operate in a marine environment where exposure to salt-water spray – known to corrode aluminum alloys – is

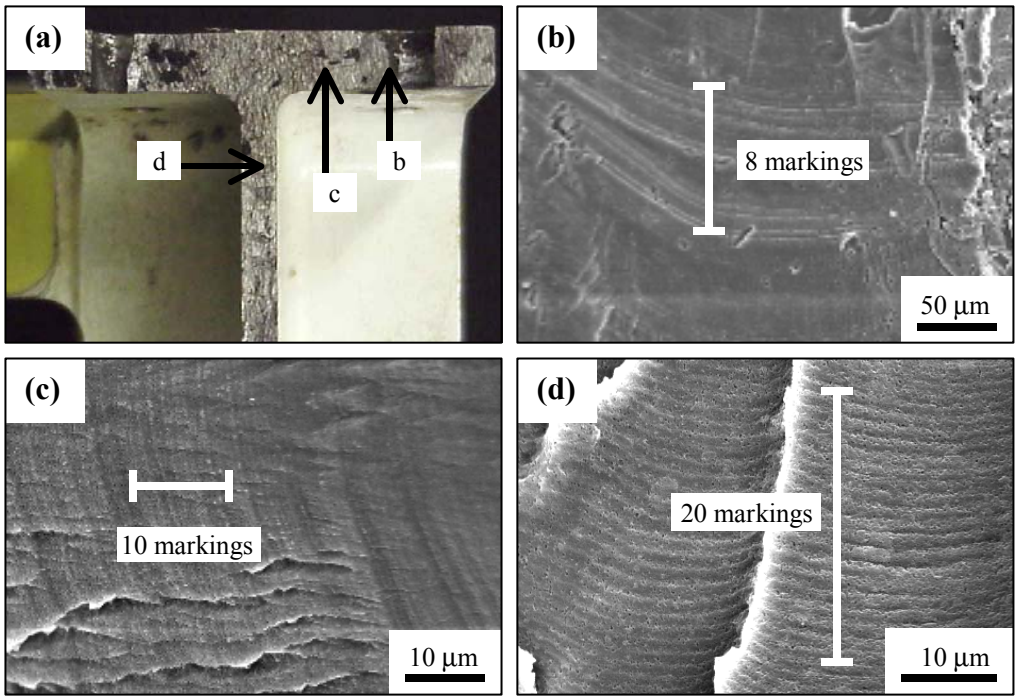

Figure 9. Micrographs of crack-surface markings are shown at high magnification. (a) A photograph of the crack surface in the pylon upper flange region is shown. High-magnification micrographs are shown of the crack surface (b) near the crack initiation region, (c) between the fastener hole and the web, and (d) in the pylon web.

likely. Fastener holes create a crevice-like environment that entraps water resulting in a corrosive environment where pitting is likely (ref. 12). Pitting damage is difficult to detect because the damage is highly localized (*e.g*. may be hidden in a fastener hole) and only affects a small amount of material.

The crack found in the fuel-tank pylon initiated at corrosion pits in the region where the highest stresses were expected. As shown in Figure 2a, vertical-downward loading on the pylon creates a high-stress region in the corner where the cantilever meets the vertical portion of the pylon. The stress concentration effect of fastener holes in this region further increases the local stress state near these discontinuities (ref. 13). Finally, corrosion pitting in these fastener holes creates rough surfaces that further increase the severity of the local stress state (refs. 14-16). Due to these three factors (pylon loading, fastener hole geometry, and corrosion pits) the highest local stress occurred at the fastener hole of Figure 3b, the crack initiation site.

Deformation markings on the crack surface were used to identify the crack initiation site. However, care must be taken when using fatigue striations to quantify the fatigue crack growth rate. Researchers have suggested that a single striation may not be the result of a single load cycle (refs. 7, 8). Unpublished research for aluminum alloys by Piascik has revealed similar findings; Paris regime fatigue crack growth ($\Delta K > 7$ MPa$\sqrt{m}$) exhibits single load cycle per striation behavior, but near the fatigue crack growth threshold ($\Delta K < 5$ MPa$\sqrt{m}$) multiple load cycles are required per striation because more complex crack-tip damage processes are operative. As the crack propagated through the webbing, clear evidence of striation markings was found on the crack surface indicating a fatigue crack growth rate of approximately 10^{-6} m/cycle (recall Figure 9d). Test data for similar materials indicates this occurs for values of ΔK between 15 MPa$\sqrt{m}$ and 20 MPa$\sqrt{m}$; in the range of ΔK where each load cycle is expected to produce one striation. Striations in Figures 9b and 9c were not well defined possibly because the values of ΔK were low, *i.e*. near the fatigue crack growth threshold.

The striation markings seen in Figure 9d indicate that rapid crack propagation occurred in the pylon webbing (approximately 1.5 mm of crack growth per 1000 load cycles). As the crack grew, increases in ΔK and fatigue crack growth rates likely occurred. Pylon failure was prevented because a vertical stiffener deflected the crack causing crack arrest. Cracks tend to propagate in the direction perpendicular to the principal (largest) normal stress, the orientation where the mode I stress intensity factor (K_I) is at its maximum value and the mode II stress intensity factor (K_{II}) is zero (ref. 17). This stiffener likely diverted the crack from principal stress directions, resulting in mixed-mode crack-tip loading (*i.e.* both K_I and K_{II} are non-zero) and a reduction in K_I, the crack driving force. Crack arrest was likely a result of a reduction in crack driving force and crack-face contact due to mode II (sliding-mode) displacements further reducing the fatigue crack driving force (refs. 18, 19). The crack surface corrosion product in Figure 5 was likely produced by sliding-mode contact of rough crack surfaces.

Failure of this pylon was prevented when the vertical stiffener diverted and arrested the propagating fatigue crack. However, prevention of similar cracking problems in the future should focus on preventing the corrosion pitting that lead to crack initiation. In other words, preventing crack initiation (here caused by corrosion pitting) is preferable to, and likely more successful than, relying on techniques to arrest cracks after they develop.

Conclusions

A failure analysis was performed to determine the cause of an eight-inch-long crack found in a U.S. Coast Guard HH-60 helicopter external fuel-tank pylon. Based on the failure analysis results presented in this paper, it is believed the following sequence of events occurred and resulted in the crack.

1. **Corrosion pitting** – The initial damage occurred when corrosion pits formed in a fastener hole. Fasteners are known to provide a crevice-like environment where entrapped water can form a highly corrosive environment where pitting is likely to occur.

2. **Crack initiation** – Crack initiation occurred in a region of high local stress; at corrosion pits in a fastener hole, near the corner with the highest bending stress; all three factors greatly increases local state of stress.

3. **Fatigue crack propagation** – Crack-surface markings indicate that crack propagation was a result of fatigue, or cyclic, loading. Corrosion products on the crack surfaces suggest that fatigue crack growth occurred in a corrosive environment. The presence of fatigue loading and corrosive environment exacerbates cracking; fatigue cracks contained in 7000 series alloys exposed to air with 90% humidity will continue to grow at extremely low loads.

4. **Crack arrest** – After propagating through approximately 80% of the pylon web, the crack intersected a vertical stiffener and was diverted. Diverting the crack likely lowered the crack-tip driving force resulting in crack arrest.

References

1. J.W. Lincoln, "Damage Tolerance for Helicopters," *Aeronautical Fatigue in the Electronic Era*, Proceedings of the 15th Symposium of the International Committee on Aeronautical Fatigue, 21-23 June, 1989, Jerusalem, Israel, A. Berkovits, Ed., 1989, pp. 263-290.

2. R.A. Everett, Jr. and W. Elber, "Damage Tolerance Issues Related to Metallic Rotorcraft Dynamic Components," *Journal of the American Helicopter Society*, Vol. 45, 2000, pp. 3-10.

3. R.P. Gangloff, "Corrosion Fatigue Crack Propagation in Metals," *Environment-Induced Cracking of Metals*, NACE-10, R. P. Gangloff and M. B. Ives, Eds., National Association of Corrosion Engineers, 1990, pp. 55-109.

4. S. Suresh, A.K. Vasudevan, and P.E. Bretz, "Mechanisms of Slow Fatigue Crack Growth in High Strength Aluminum Alloys: Role of Microstructure and Environment," *Metallurgical Transactions*, Vol. 15A, 1984, pp. 369-379.

5. A.K. Vasudevan and S. Suresh, "Influence of Corrosion Deposits on Near-Threshold Fatigue Crack Growth Behavior in 2XXX and 7XXX Series Aluminum Alloys," *Metallurgical Transactions*, Vol. 13A, 1982, pp. 2271-2280.

6. C. Laird, "The Influence of Metallurgical Structure an the Mechanisms of Fatigue Crack Propagation," *Fatigue Crack Propagation, ASTM STP 415*, American Society for Testing and Materials, Philadelphia, PA, 1967, pp. 131-168.

7. D.L. Davidson and J. Lankford, "Fatigue Crack Growth in Metals and Alloys: Mechanisms and Micromechanisms," *International Materials Reviews*, Vol. 37, 1992, pp. 45-76.

8. H.J. Roven, M.A. Langoy, and E. Nes, "Striations and the Fatigue Crack Growth Mechanism in a Micro-Alloyed Steel," *Fatigue '87*, Vol. 1, R.O. Ritchie and E.A. Starke, Eds., Warley: Engineering Materials Advisory Services, pp. 175-184.

9. J. Schijve, "The Significance of Fractography for Investigations of Fatigue Crack Growth Under Variable-Amplitude Loading," *Fatigue and Fracture of Engineering Materials and Structures*, Vol. 22, 1999, pp. 87-99.

10. P.E. Bretz, R.J. Bucci, R.C. Malcolm, and A.K. Vasudevan, "Constant-Amplitude Fatigue Crack Growth Behavior of 7XXX Aluminum Alloys," *Fracture Mechanics: Fourteenth Symposium – Volume II: Testing and Applications, ASTM STP 791*, J.C. Lewis and G. Sines, Eds., American Society for Testing and Materials, Philadelphia, PA, 1983, pp. II-67-II-86.

11. C.S. Oh, and J.H. Song, "Crack Growth and Closure Behavior of Surface Cracks Under Pure Bending Loading," *International Journal of Fatigue*, Vol. 23, 2001, pp. 251-258.

12. M.G. Fontana, *Corrosion Engineering*, 3rd Ed., 1986, McGraw Hill, New York, pp. 51-73.

13. S. Suresh, *Fatigue of Materials*, 1991, Cambridge University Press, pp. 272-290.

14. P.S. Pao, S.J. Gill, and C.R. Feng, "On Fatigue Crack Initiation From Corrosion Pits in 7075-T7351 Aluminum Alloy," *Scripta Materiallia*, Vol. 43, 2000, pp. 391-396.

15. K.K. Sankaran, R. Perez, and K.V. Jata, "Effects of Pitting Corrosion on the Fatigue Behavior of Aluminum Alloy 7075-T6: Modeling and Experimental Studies," *Materials Science and Engineering*, Vol. A297, 2001, pp. 223-229.

16. G.S. Chen, K.C. Wan, M. Gao, R. P. Wei, and T.H. Flournoy, "Transition from Pitting to Fatigue Crack Growth – Modeling of Corrosion Fatigue Crack Nucleation in a 2024-T3 Aluminum Alloy," *Materials Science and Engineering*, Vol. A219, 1996, pp. 126-132.

17. F. Erdogan and G.C. Sih, "On the Crack Extension in Plates Under Plane Loading and Transverse Shear," *Journal of Basic Engineering*, December 1963, pp. 519-527.

18. E.K. Tschegg, "Sliding Mode Crack Closure and Mode III Fatigue Crack Growth in Mild Steel," *Acta Metallurgica*, Vol. 31, 1983, pp. 1323-1330.

19. X. Yu and A. Abel, "Mixed-mode Crack Surface Interference Under Cyclic Shear Loads," *Fatigue and Fracture of Engineering Materials and Structures*, Vol. 23, 2000, pp. 151-158.

REPORT DOCUMENTATION PAGE

Form Approved
OMB No. 0704-0188

Public reporting burden for this collection of information is estimated to average 1 hour per response, including the time for reviewing instructions, searching existing data sources, gathering and maintaining the data needed, and completing and reviewing the collection of information. Send comments regarding this burden estimate or any other aspect of this collection of information, including suggestions for reducing this burden, to Washington Headquarters Services, Directorate for Information Operations and Reports, 1215 Jefferson Davis Highway, Suite 1204, Arlington, VA 22202-4302, and to the Office of Management and Budget, Paperwork Reduction Project (0704-0188), Washington, DC 20503.

1. AGENCY USE ONLY (*Leave blank*)

2. REPORT DATE
April 2002

3. REPORT TYPE AND DATES COVERED
Technical Memorandum

4. TITLE AND SUBTITLE
Failure Analysis of a Helicopter External Fuel-Tank Pylon

5. FUNDING NUMBERS
WU 706-61-11-03

6. AUTHOR(S)
John A. Newman, Robert S. Piascik, and Richard A. Lindenberg

7. PERFORMING ORGANIZATION NAME(S) AND ADDRESS(ES)
NASA Langley Research Center
Hampton, VA 23681-2199

U.S. Army Research Laboratory
Vehicle Technology Directorate
NASA Langley Research Center
Hampton, VA 23681-2199

8. PERFORMING ORGANIZATION REPORT NUMBER
L-18164

9. SPONSORING/MONITORING AGENCY NAME(S) AND ADDRESS(ES)
National Aeronautics and Space Administration
Washington, DC 20546-0001
and
U.S. Army Research Laboratory
Adelphi, MD 20783-1145

10. SPONSORING/MONITORING AGENCY REPORT NUMBER
NASA/TM-2002-211645
ARL-TR-2711

11. SUPPLEMENTARY NOTES

12a. DISTRIBUTION/AVAILABILITY STATEMENT
Unclassified-Unlimited
Subject Category 26 Distribution: Standard
Availability: NASA CASI (301) 621-0390

12b. DISTRIBUTION CODE

13. ABSTRACT *(Maximum 200 words)*
An eight-inch-long (0.2 m) crack was found in an external fuel-tank pylon of a U.S. Coast Guard HH-60 helicopter. The damaged pylon was removed from service and destructively examined at NASA Langley Research Center (LaRC) to determine the cause of the crack. Results of the analysis revealed that crack initiation occurred at corrosion pits in a fastener hole and crack propagation was a result of cyclic loading.

14. SUBJECT TERMS
Failure analysis, corrosion pits, fatigue crack growth, crack surface analysis, helicopter pylon, aluminum

15. NUMBER OF PAGES
16

16. PRICE CODE

17. SECURITY CLASSIFICATION OF REPORT
Unclassified

18. SECURITY CLASSIFICATION OF THIS PAGE
Unclassified

19. SECURITY CLASSIFICATION OF ABSTRACT
Unclassified

20. LIMITATION OF ABSTRACT
UL